of the square coaxial line $(a = b, s = t, t_1 = t_2 = 0)$ as the number of basis functions $N_1 = N_2$ is increased. In the last line of Table I the exact values for the square coaxial line are listed as quoted from [2]. One may observe that the values of Z_0 tend to increase with an increasing number of basis functions, such that as $N_1 \to \infty$ the value of Z_0 as computed here increases monotonically toward the exact value.

For the case of the rectangular coaxial line, computed with $N_1 = N_2 = 20$, the authors' results coincide with those from [5]. Fig. 2 shows the characteristic impedance as a function of the height of the inner conductor t, with various other parameters. These figures can be used for design purposes when transitions between ridged waveguides and coaxial lines are needed.

References

[1] J. C. Dix, "Design of waveguide/coaxial transition for the band 2.5-4.1 Gc/s," *Proc. Inst. Elect. Eng.*, vol. 110, no. 2, pt. H, pp. 253-255, Feb. 1963.

[2] M. A. R. Gunston, *Microwave Transmission Line Impedance Data*. New York: Van Nostrand, 1972

[3] E. A. Navarro, V. Such, B. Gimeno, and J. L. Cruz, "T-junctions in square coaxial waveguide: An FD-TD approach," *IEEE Trans. Microwave Theory Tech.*, vol. 42, pp. 347-350, Feb. 1994.

[4] A. Matsumoto, Ed., *Microwave Filters and Circuits. Supplement 1 to Advances in Microwaves*. New York: Academic Press, 1970, ch. 5.

[5] W. S. Metcalf, "Characteristic impedance of rectangular transmission lines," *Proc. Inst. Elect. Eng.*, vol. 112, no. 11, pt. H, pp. 2033-2039, Nov. 1965.

[6] H. J. Riblet, "Upper limits on the error of an improved approximation for the characteristic impedance of rectangular coaxial line," *IEEE Trans. Microwave Theory Tech.*, vol. MTT-28, pp. 666-667, June 1980.

Propagation Characteristics of a Dielectric-Coated Coaxial Helical Waveguide in a Lossy Medium

Takahiro Iyama and Jun-ichi Takada

***Abstract*—In this paper, the authors discuss the propagation characteristics of a dielectric-coated coaxial helical waveguide in a lossy medium. The authors place emphases on the phase constant, propagation modes, magnetic fields distribution, and attenuation constant. When permittivity of the internal region is relatively small, two propagation modes exist and dominant components of their magnetic fields are different. Lastly, the authors discuss the relation between the attenuation constant and permittivities.**

***Index Terms*—Absorbing media, helical waveguide, hyperthermia.**

I. Introduction

Coaxial helical waveguides have been studied by Hill and Wait [1], Wait [2], Mirotznik *et al.* [3], and other researchers. In those papers, the bared or noncoated helices were discussed. In this paper, the authors discuss the theoretical propagation characteristics of a dielectric-coated coaxial helical waveguide in a lossy medium. This structure corresponds to the coaxial helical applicator for microwave hyperthermia which is covered with a catheter.

Manuscript received November 22, 1996; revised December 24, 1996

The authors are with the International Cooperation Center for Science and Technology, Tokyo Institute of Technology, Meguro-ku, Tokyo 152 Japan.

Publisher Item Identifier S 0018-9480(97)02536-2.

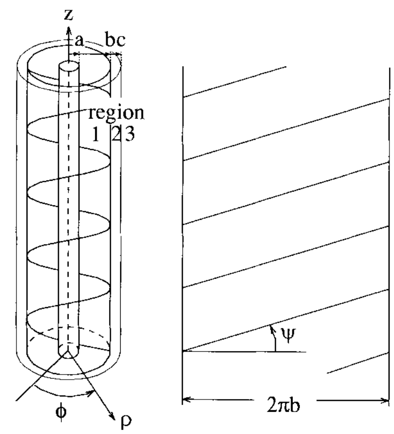

Fig. 1. Perspective view of a dielectric-coated coaxial helical waveguide constructed of three layers.

II. Formulation

The analysis model is shown in Fig. 1. The inner conductor of radius a is perfectly conducting, and the helical wire is wound at $\rho = b$ with pitch angle ψ. The model is divided into three regions as:

$$a < \rho < b\text{: region } 1 \text{ (permittivity } \varepsilon_1)$$
$$b < \rho < c\text{: region } 2 \text{ (permittivity } \varepsilon_2)$$
$$c < \rho\text{: region } 3 \text{ (permittivity } \varepsilon_3).$$

The permeability μ_0 is constant for all regions. The authors assume that the variations of the electric and magnetic fields in the z-direction is $\exp(-\gamma \cdot z)$ and those in the ϕ-direction is constant; γ is the complex propagation constant along the z-direction. At $\rho = b$, the boundary conditions are represented by the sheath helix model, i.e., the cylindrical surface at $\rho = b$ is assumed to have anisotropic conductivity that the surface current can flow along only the ψ-direction. With those assumptions, the authors obtain the following Maxwell's equations in the cylindrical coordinates:

$$\frac{\partial^2 H_z}{\partial \rho^2} + \frac{1}{\rho}\frac{\partial H_z}{\partial \rho} + (\omega^2 \varepsilon \mu_0 + \gamma^2) H_z = 0 \tag{1}$$

$$E_\phi = \frac{j\omega\mu_0}{\omega^2 \varepsilon \mu + \gamma^2}\frac{\partial H_z}{\partial \rho} \tag{2}$$

$$\frac{\partial^2 E_z}{\partial \rho^2} + \frac{1}{\rho}\frac{\partial E_z}{\partial \rho} + (\omega^2 \varepsilon \mu_0 + \gamma^2) E_z = 0 \tag{3}$$

$$H_\phi = -\frac{j\omega\varepsilon}{\omega^2 \varepsilon \mu_0 + \gamma^2}\frac{\partial E_z}{\partial \rho} \tag{4}$$

where ω is the angular frequency. The appropriate solutions in region 1 and 2 are

$$H_z = A_i I_0(\kappa_i \rho) + B_i K_0(\kappa_i \rho) \tag{5}$$

$$E_\phi = -\frac{j\omega\mu}{{\kappa_i}^2}[A_i I_0'(\kappa_i \rho) + B_i K_0'(\kappa_i \rho)] \tag{6}$$

$$E_z = A_i^* I_0(\kappa_i \rho) + B_i^* K_0(\kappa_i \rho) \tag{7}$$

$$H_\phi = \frac{j\omega\varepsilon_i}{{\kappa_i}^2}[A_i^* I_0'(\kappa_i \rho) + B_i^* K_0'(\kappa_i \rho)], \qquad i = 1, 2 \tag{8}$$

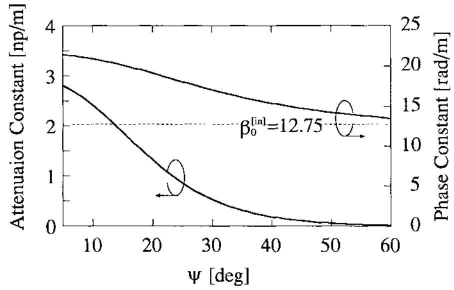

Fig. 2. Propagation constant of fast wave mode: $f = 430$ MHz, $a = 0.185$ mm, $b = 0.6$ mm, $c = 0.8$ mm, $\varepsilon_{r1} = 2$, $\varepsilon_{r2} = 2$, and $\varepsilon_{r3} = 53 - j59$.

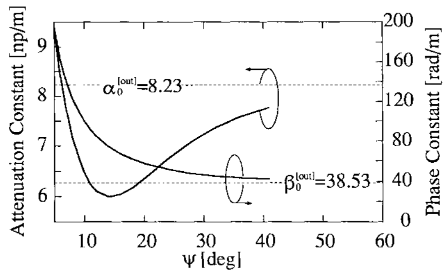

Fig. 3. Propagation constant of slow wave mode: $f = 430$ MHz, $a = 0.185$ mm, $b = 0.6$ mm, $c = 0.8$ mm, $\varepsilon_{r1} = 2$,$\varepsilon_{r2} = 2$, and $\varepsilon_{r3} = 53 - j59$.

and in region 3

$$H_z = A_3 K_0(\kappa_3 \rho) \tag{9}$$

$$E_\phi = -\frac{j\omega\mu}{{\kappa_3}^2} A_3 K_0^{'}(\kappa_3 \rho) \tag{10}$$

$$E_z = A_3^* K_0(\kappa_3 \rho) \tag{11}$$

$$H_\phi = \frac{j\omega\varepsilon_3}{{\kappa_3}^2} A_3^* K_0^{'}(\kappa_3 \rho) \tag{12}$$

where $\kappa_i = \sqrt{-(\omega^2 \varepsilon_i \mu_0 + \gamma^2)}$ $(i = 1, 2, 3)$. The boundary conditions at $\rho = a$ are

$$E_z(a) = E_\phi(a) = 0 \tag{13}$$

and at $\rho = b$ are

$$H_z(b_{-0}) = H_z(b_{+0}) + j_\phi \tag{14}$$

$$E_\phi(b_{-0}) = E_\phi(b_{+0}) \tag{15}$$

$$E_z(b_{-0}) = E_z(b_{+0}) \tag{16}$$

$$H_\phi(b_{-0}) = H_\phi(b_{+0}) - j_z \tag{17}$$

$$E_l(b_{-0}) = E_\phi(b_{-0}) \cos\psi + E_z(b_{-0}) \sin\psi = 0 \tag{18}$$

where the current on the sheath helix is $I_t = 2\pi b j_z / \sin\psi = 2\pi b j_\phi / \cos\psi$, and at $\rho = c$

$$E_z(c_{-0}) = E_z(c_{+0}) \tag{19}$$

$$H_\phi(c_{-0}) = H_\phi(c_{+0}) \tag{20}$$

$$H_z(c_{-0}) = H_z(c_{+0}) \tag{21}$$

$$E_\phi(c_{-0}) = E_\phi(c_{+0}). \tag{22}$$

To satisfy all the boundary conditions, the following eigenvalue equation for γ is derived:

$$-\frac{j\omega\mu}{{\kappa_1}^2} A_1 (I_0^{'}(\kappa_1 b) - P_1 K_0^{'}(\kappa_1 b)) \cos\psi + A_1^* (I_0(\kappa_1 b) - P_1^* K_0(\kappa_1 b)) \sin\psi = 0. \tag{23}$$

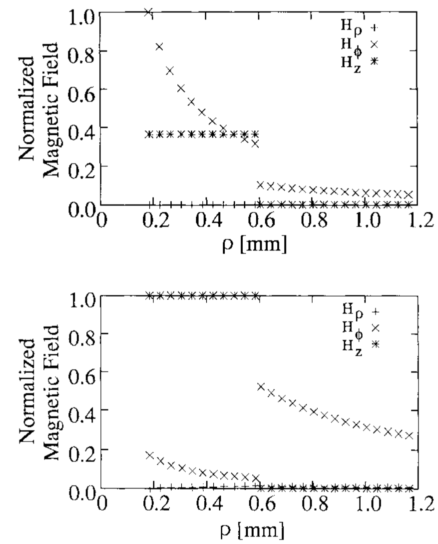

Fig. 4. Magnetic field's distribution of fast and slow wave modes: $a = 0.185$ mm, $b = 0.6$ mm, $c = 0.8$ mm, $\varepsilon_{r1} = 2$, $\varepsilon_{r2} = 2$, $\varepsilon_{r3} = 53 - j59$, and pitch angle $\psi = 45°$.

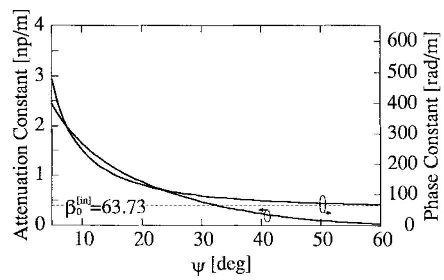

Fig. 5. Propagation constant of fast wave mode:$f = 430$ MHz, $a = 0.185$ mm, $b = 0.6$ mm, $c = 0.8$ mm, $\varepsilon_{r1} = 50$, $\varepsilon_{r2} = 2$, and $\varepsilon_{r3} = 53 - j59$.

Definitions of A and P are given in the Appendix. The solution of the equation (the eigenvalue) is the propagation constant γ. In general γ is complex; the real part of γ is the attenuation constant α and the imaginary part is the phase constant β. Equation (23) is solved by the secant method. The validity of (23) for $\varepsilon_{r2} = \varepsilon_{r3}$ is confirmed by comparison with the results shown in [3].

III. Numerical Results

Figs. 2 and 3 show the attenuation constant α and the phase constant β as functions of the pitch angle ψ, for $\varepsilon_{r1} = 2$, $\varepsilon_{r2} = 2$, and $\varepsilon_{r3} = 53 - j59$. For this structure, two independent eigenvalues exist. Fig. 4 shows the magnetic field's distribution of both modes in the ρ-direction. In the internal region, H_ϕ is dominant for the fast wave mode, and H_z is dominant for the slow wave mode. The asymptotic values to $\psi \to 90°$ correspond to one for the internal coaxial guide (region 1) and one for the external Goubau waveguide (regions 2 and 3, respectively). If this coaxial helical waveguide is fed by the ordinary coaxial waveguide, fast wave mode is dominantly excited.

Fig. 5 shows the attenuation and phase constants when $\varepsilon_{r1} = 50$. In this case, only one eigenvalue exists and the asymptotic value is one for the coaxial waveguide (region 1).

Fig. 6 shows the propagation constant as a function of ε_{r1} for fixed ψ. When the phase constant of the coaxial guide (region 1) is nearly equal to that of the Goubau guide (regions 2 and 3, respectively), the attenuation constant is maximum. In this case, strong coupling is expected.

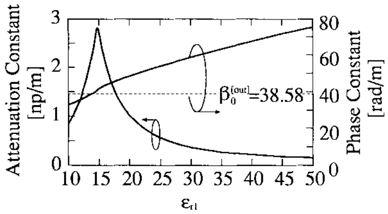

Fig. 6. Propagation constant as a function of the permittivity ε_{r1}: $f = 430$ MHz, $a = 0.185$ mm, $b = 0.6$ mm, $c = 0.8$ mm, $\varepsilon_{r2} = 2$, $\varepsilon_{r3} = 53 - j59$, and pitch angle $\psi = 45°$.

IV. Conclusion

The authors calculated the propagation constant of a dielectric-coated coaxial helical waveguide in a lossy medium. In the case where the internal permittivity ε_1 is small, two modes exist and are related with the internal or external construction, respectively, and wavelength reduction is remarkable in the external–dominant mode. In the case where the internal permittivity ε_1 is large, the wavelength reduction is dominated by the inner dielectric, and when the phase constant of the coaxial guide (region 1) is nearly equal to that of the Goubau guide (regions 2 and 3, respectively), the attenuation constant becomes large. The calculation for the practical applicator with finite length is left for future study.

Appendix

Definitions of A and P:

$$A_1 = \frac{1}{R} I_t \cos\psi, \quad A_1^* = -\frac{1}{R^*} I_t \sin\psi$$

$$P_1 = \frac{I_0'(\kappa_1 a)}{K_0'(\kappa_1 a)}, \quad P_1^* = \frac{I_0(\kappa_1 a)}{K_0(\kappa_1 a)}$$

$$P_2 = \frac{{\kappa_2}^2 I_0(\kappa_2 c) K_0'(\kappa_3 c) - {\kappa_3}^2 I_0'(\kappa_2 c) K_0(\kappa_3 c)}{{\kappa_2}^2 K_0(\kappa_2 c) K_0'(\kappa_3 c) - {\kappa_3}^2 K_0'(\kappa_2 c) K_0(\kappa_3 c)}$$

$$P_2^* = -\frac{\varepsilon_3 {\kappa_2}^2 I_0(\kappa_2 c) K_0'(\kappa_3 c) - \varepsilon_2 {\kappa_3}^2 I_0'(\kappa_2 c) K_0(\kappa_3 c)}{\varepsilon_3 {\kappa_2}^2 K_0(\kappa_2 c) K_0'(\kappa_3 c) - \varepsilon_3 {\kappa_3}^2 K_0'(\kappa_2 c) K_0(\kappa_3 c)}$$

$$P_3 = \frac{{\kappa_3}^2 I_0(\kappa_2 c) K_0'(\kappa_2 c) - {\kappa_3}^2 I_0'(\kappa_2 c) K_0(\kappa_2 c)}{{\kappa_3}^2 K_0(\kappa_3 c) K_0'(\kappa_2 c) - {\kappa_2}^2 K_0'(\kappa_3 c) K_0(\kappa_2 c)}$$

$$P_3^* = \frac{\varepsilon_2 {\kappa_3}^2 I_0(\kappa_2 c) K_0'(\kappa_2 c) - \varepsilon_2 {\kappa_3}^2 I_0'(\kappa_2 c) K_0(\kappa_2 c)}{\varepsilon_2 {\kappa_3}^2 K_0(\kappa_3 c) K_0'(\kappa_2 c) - \varepsilon_3 {\kappa_2}^2 K_0'(\kappa_3 c) K_0(\kappa_2 c)}$$

$$Q = \frac{{\kappa_2}^2 (I_0'(\kappa_1 b) - P_1 K_0'(\kappa_1 b))}{{\kappa_1}^2 (I_0'(\kappa_2 b) - P_2 K_0'(\kappa_2 b))}$$

$$Q^* = \frac{I_0(\kappa_1 b) - P_1^* K_0(\kappa_1 b)}{I_0(\kappa_2 b) - P_2^* K_0(\kappa_2 b)}$$

$$R = I_0(\kappa_1 b) - P_1 K_0(\kappa_1 b) - Q(I_0(\kappa_2 b) - P_2 K_0(\kappa_2 b))$$

$$R^* = j\omega \left(\frac{\varepsilon_1}{{\kappa_1}^2} (I_0'(\kappa_1 b) - P_1^* K_0'(\kappa_1 b)) - Q^* \frac{\varepsilon_2}{{\kappa_2}^2} (I_0'(\kappa_2 b) - P_2^* K_0'(\kappa_2 b)) \right)$$

References

[1] D. A. Hill and J. R. Wait, “Propagation along a coaxial cable with a helical shield,” *IEEE Trans. Microwave Theory Tech.*, vol. MTT-28, pp. 84–89, Feb. 1980.

[2] J. R. Wait, “Electromagnetic theory of the loosely braided coaxial Cable: Part I,” *IEEE Trans. Microwave Theory Tech.*, vol. MTT-24, pp. 547–553, Feb. 1976.

[3] M. S. Mirotznik, N. Engheta, and K. R. Foster, “Heating characteristics of thin helical antennas with conducting cores in a lossy medium—I: Noninsulated antennas,” *IEEE Trans. Microwave Theory Tech.*, vol. 41, pp. 1878–1886, Nov. 1993.

[4] R. E. Collin, *Field Theory of Guided Waves*, 2nd ed. Piscataway, NJ: IEEE Press, 1991, pp. 718–720.